Sex- and region-specific differences in microglia phenotype and characterization of the peripheral immune response following early-life infection in neonatal male and female rats

Brittany F. Osborne[a,*], **Alexandra Turano**[a], **Jasmine I. Caulfield**[a], and **Jaclyn M. Schwarz**[a]

[a]University of Delaware, Department of Psychological and Brain Sciences, 108 Wolf Hall, Newark, DE, 19716, USA.

Abstract

Early-life infection has been shown to have profound effects on the brain and behavior across the lifespan, a phenomenon termed "early-life programming". Indeed, many neuropsychiatric disorders begin or have their origins early in life and have been linked to early-life immune activation (e.g. autism, ADHD, and schizophrenia). Furthermore, many of these disorders show a robust sex bias, with males having a higher risk of developing early-onset neurodevelopmental disorders. The concept of early-life programming is now well established, however, it is still unclear how such effects are initiated and then maintained across time to produce such a phenomenon. To begin to address this question, we examined changes in microglia, the immune cells of the brain, and peripheral immune cells in the hours immediately following early-life infection in male and female rats. We found that males showed a significant decrease in BDNF expression and females showed a significant increase in IL-6 expression in the cerebellum following *E.coli* infection on postnatal day 4; however, for most cytokines examined in the brain and in the periphery we were unable to identify any sex differences in the immune response, at least at the time points examined. Instead, neonatal infection with *E.coli* increased the expression of a number of cytokines in the brain of both males and females similarly including TNF-α, IL-1β, and CD11b (a marker of microglia activation) in the hippocampus and, in the spleen, TNF-α and IL-1β. We also found that protein levels of GRO- KC, MIP-1a, MCP1, IP-10, TNF-α, and IL-10 were elevated 8-hours postinfection, but this response was resolved by 24-hours. Lastly, we found that males have more thin microglia than females on P5, however, neonatal infection had no effect on any of the microglia morphologies we examined. These data show that sex differences in the acute immune response to neonatal infection are likely gene, region, and even time dependent. Future research should consider these factors in order to develop a comprehensive understanding of the immune response in males and females as these changes are likely the initiating agents that lead to the long-term, and often sex-specific, effects of early-life infection.

aturano@psych.udel.edu, joc5376@psu.edu, jschwarz@psych.udel.edu. *Corresponding Author: Brittany F. Osborne, University of Delaware, 108 Wolf Hall, Newark, DE 19716, bosborne@psych.udel.edu.

Keywords

1. Introduction

Microglia are the resident immune cells of the brain and the immune molecules they produce, including cytokines and chemokines, have profound effects on neural function and behavior. During early brain development, microglia migrate into the brain from the periphery where they release cytokines and chemokines important for brain development [1–5]. Microglia have a critical role in many neurodevelopmental processes such as axon guidance, neurite growth, synaptic pruning, and apoptosis [4,6–10] making them important regulators of synapse function, plasticity, and circuit formation throughout early brain development and even beyond [11–14]. It has been proposed that abnormalities in, or dysregulation of, these critical microglial-neuronal interactions during early development may contribute to the neurodevelopmental deficits observed in mental health disorders such as autism, schizophrenia, and depression [15,16]. Indeed, many of these disorders are present early in life or have their origins in early-life experience, and are the largest source of years lived with disability [17].

During the first postnatal week in rats – equivalent to the third trimester of pregnancy in humans – microglia in many brain regions exhibit an amoeboid phenotype, which is followed by a gradual change in their phenotype to a more heterogeneous population (e.g., stout microglia and/or microglia with thick processes) around postnatal day (P) 4. By the end of the third postnatal week, the most predominate microglial phenotype is microglia with long, thin processes (i.e. "ramified") [2,4]. The first few weeks of postnatal development also represent a critical period for hormonally mediated sexual differentiation of the brain [18–20]. Just prior to birth, the testes produce a surge of testosterone that masculinizes the brain. The absence of this testosterone surge leads to the typical development of the "female" brain [21]. Early in development, many brain regions already display sex differences in microglia number and/or morphology including the hippocampus [22] and cerebellum [23]. Additionally on P4, males have more microglia than females in brain regions critical for learning and emotion including the hippocampus, amygdala, and cortex [2]. These same brain regions display significant sex- specific expression of cytokines and chemokines. For example, the chemokine ligands CCL20 and CCL4 are elevated 200- and 50- fold, respectively, in the hippocampus/cortex of males compared to females [2], suggesting that the surge in testosterone in males may increase the colonization of microglia and the expression of immune molecules in the developing brain in a sex-dependent manner.

Several neuropsychiatric and developmental disorders linked to early-life immune activation, such as Autism and ADHD, are also male-biased in their prevalence [15,16,24–26]; thus, males may be more vulnerable to the effects of immune activation or immune dysregulation early in life. Indeed, there is evidence to suggest that males often have poorer long-term outcomes following early-life immune activation compared to females [27–29]; however,

very little research has examined the immediate changes in microglia or the immune molecules they produce, and how these changes may differ between males and females. Such differences may underlie the increased vulnerability of males to the long-term, negative consequences of early-life immune activation. Thus, the goal of this study was to determine the acute changes in microglia function and morphology, as well as changes in the peripheral immune response, in the first 24 hours following early-life infection on P4 in male and female rats.

2. Materials and Methods

2.1 Animals and Breeding

Adult male and female Sprague Dawley rats were ordered from Envigo Laboratories in Indianapolis, Indiana. Rats were housed in same sex pairs in clear, polyethylene cages (45cm x 20.5cm x 24cm) and allowed one week of acclimation to the facility prior to breeding. The colony room was maintained at 22°C on a 12:12 hr light:dark cycle (lights on at 7:00 a.m.) and all rats had *ad-libitum* access to food and water. For breeding, male and female pairs were housed together for five days and the presence of sperm plugs was checked daily to determine the date of embryonic day one (E1). Pregnant females were housed individually two days prior to the calculated date of birth (P0). Litter sizes and male to female ratios were not adjusted at the time of birth; however, no more than 1–2 pups from a given litter were represented in each experimental group to minimize possible litter effects. Sentinel rats were housed in the colony room and periodically examined for the presence of common rodent diseases. All tests came back negative. All experiments were approved by the University of Delaware Institutional Animal Care and Use Committee.

2.2 Bacterial Culture and Neonatal Infection

Prior to the start of the study, *Escherichia coli* (E.coli; ATCC 1547; American Type Culture Collection, Manassas, VA) culture vial contents were hydrated and grown overnight at 37°C in 30 ml of brain-heart infusion (BHI). Cultures were aliquoted in 1 ml stock samples, supplemented with 10% glycerol and stored at −20°C. For injections, a stock culture was thawed and incubated 19–24 hours in 40 ml of BHI at 37°C. The culture was removed from incubation, the number of bacteria present was determined by a microplate reader (BioTek; model ELx808), and the number of colony forming units (CFU) was quantified by extrapolating from previously determined growth curves. Cultures were centrifuged at 300g for 15 minutes, supernatants were discarded, and the bacteria were re-suspended in the appropriate volume of sterile, pyrogen- free, Dulbecco's phosphate buffered saline (DPBS) for a final concentration of 1×10^6 CFU of live bacterial *E. coli*. On P4, pups were removed from the dam, counted, sexed (based on anogenital distance), and administered a subcutaneous injection of either 0.1 ml of 1×10^6 CFU of *E.coli* or 0.1 ml of sterile DPBS and returned to the dam within 5 minutes. All pups in a litter were injected with the same treatment to avoid the possibility of within-litter cross-contamination from *E. coli* infection. All neonatal injections took place on P4 between 8:00 a.m. and 11:00 a.m. or 2:00 p.m. and 5:00 p.m and was balanced across all conditions for each post-infection time point.

2.3 Euthanasia for Tissue and Whole Blood Collection

Eight- or 24-hours (i.e. P5) after saline or *E.coli* injections, male and female pups (8hr: $N =$ 39, 8–10/group; 24hr: $N =$ 37, 8–10/group) were euthanized by rapid decapitation. Trunk blood was immediately collected and centrifuged at 4°C for 15 minutes at 11,900RPM for the analysis of serum. Whole hippocampus, cerebellum, and spleen were dissected on ice and flash frozen on dry ice. Tissue and serum samples were stored at −80°C until further analysis.

2.4 Quantitative Real-time PCR

RNA was extracted from frozen tissue samples using Isol-RNA Lysis Reagent (Cat. No. 2302700, 5 Prime). Genomic DNA was eliminated and cDNA (1000ng/μL) was synthesized from extracted RNA using the QuantiTect® Reverse Transcription Kit (Cat. No. 205314, Qiagen). Relative gene expression was quantified by real-time PCR using the RealMasterMixTM Fast SYBR Kit (Cat. No. 2200830, 5 Prime) in 10μL reactions on a CFX96Touch real time PCR machine. Interleukin-6 (IL-6) was analyzed using a QuantiTect® Primer Assay (Cat. No. QT00182896) and diluted according to protocol. All other primers were ordered through Integrated DNA Technologies and diluted to a final concentration of 0.13 μM (GAPDH, IL-1β, TNF-α, CD11b, Iba1, and BDNF; See Table 1 for a list of primer sequences). GAPDH was used as the housekeeping gene for all experimental groups as it did not differ significantly by sex, infection, or time point. Samples were numbered, blinded to treatment group, and run in duplicate on real-time PCR plates. For each reaction, the average quantitative threshold amplification cycle number (Cq) value was determined from each duplicate, and the $2^{-\Delta\Delta Cq}$ method was used to calculate the relative gene expression for each gene of interest relative to the housekeeping gene.

2.5 Multiplex Analysis of Serum Inflammatory Cytokines and Chemokines

The protein levels of GRO-KC (IL-8), MIP-1a (CCL3), MCP-1 (CCL2), IP-10 (CXCL10), IL-1β, IL-6, TNFα, and IL-10 in undiluted serum were analyzed at 8- and 24-hours after P4 saline or *E.coli* injections using a multiplex assay (Milliplex® Rat analyte kit). Samples were numbered and blinded to treatment group.

2.6 Tissue Collection and Immunohistochemistry for Microglia Counts

Twenty-four hours following P4 saline or *E.coli* injections, male and female pups (N = 20, 5/group) were euthanized by rapid decapitation, brains were collected on ice and immediately fixed in 4% ice-cold paraformaldehyde (PFA) for 24 hours at 4ºC. Brains were then transferred to fresh 4% PFA, then cryoprotected in 30% sucrose solution, and finally fresh 30% sucrose solution at 24-hour intervals and stored at 4ºC. Prior to slicing, fixed brains were submerged into a 10% gelatin solution and stored in fresh 30% sucrose solution at 4ºC until sliced.

Brains were sliced at 14 μm on a Leica cryostat at −25ºC and thaw-mounted directly onto Superfrost++ Micro Slides (VWR). After drying, the slides were stored at 4ºC until staining. Ionized calcium-binding adaptor molecule (Iba)-1 was chosen as the target protein for staining (Schwarz, Sholar, and Bilbo, 2012). Slides were washed 3 times (5 minutes each) with phosphate-buffered saline (PBS) and then incubated for 1 hour with a buffer solution

containing PBS, normal goat serum (Vector Laboratories), 30% Triton X (Fisher Scientific), and 30% H2O2 (in PBS) to block and permeabilize the tissue, and quench endogenous peroxidase. Slides were then washed and incubated with primary antibody (rabbit anti-Iba1, 1:1000; Wako Chemicals) overnight at room temperature. On day 2, the slides were washed again and incubated with a biotinylated secondary antibody (goat anti-rabbit IgG, 1:500; Vector Laboratories) for 2 hours at room temperature. After a final wash, immunostaining was identified by the streptavidin / horseradish peroxidase technique (Vectastain ABC kit; Cat. No. PK6100 Standard; Vector Laboratories), with diaminobenzidine as the chromagen (Schwarz, Sholar, and Bilbo, 2012). Finally, slides were dehydrated, coverslipped with Permount (Fisher Scientific), and stored at room temperature until analysis of cell counts.

2.7 Unbiased Stereology for Microglia Cell Counts in the Hippocampus

To successfully capture cell number across the neonatal hippocampus, 10 brain slices were selected from each rat for unbiased stereology using the Paxinos, Ashwell, and Tork Atlas of the Developing Rat Nervous System (Figures 166–176; 2nd edition;1994). Iba-1 stained cells were counted using the optical fractionator method within the StereoInvestigator program (Mouton, 2002; Glaser *et al.* 2007; Microbrightfield Inc.; Bilbo et al. 2010). The optical dissector height was set at 4 μm (with a 1-μm guard zone on top and bottom) and stained cells within each frame were manually counted under the 100× oil objective lens. For whole hippocampus counting, the contour tracing was manually drawn around the outermost portion of the whole region in both the left and right hemisphere. Similarly, for counting within individual regions of the hippocampus (CA1, CA3, and dentate gyrus), the contour tracing was manually drawn around the outermost portion of the target region within both hemispheres. Cells were only counted if the whole cell body was visible (average diameter = between 15 and 25 μm) and if the stain appeared uniformly dark and apparent throughout the cell to avoid counting cell fragments. Importantly, while perivascular macrophages may also stain positively for Iba-1, these cells only represent approximately 4% of the Iba-1 positive cell population within the brain [30] and therefore would have little, if any, influence on the counts analyzed here [2].

Volume estimates were also obtained for each contour tracing using Cavalieri's principle within the StereoInvestigator Program. Volume estimates for the target regions (whole hippocampus, CA1, CA3, or dentate gyrus) were calculated by summing the areas given by the Cavalieri estimator for each trace and then multiplying by slice thickness (14 μm) and total number of slices counted. Volume estimates were used to rule out potential differences in microglial number due only to size differences in target brain regions (see statistical analysis section).

2.8 Categorization of Microglial Morphology

Iba1-positive cells were classified into four morphological categories based on the shape and configuration of their processes: 1) round/amoeboid microglia with no processes; 2) stout microglia with short processes; 3) thick microglia with long, thick processes; and 4) thin microglia with long, thin, ramified processes. The total number of Iba-1 postive cells in each category was counted by an experimenter, blind to sex and treatment, for all representative sections of the whole hippocampus, CA1, CA3, and dentate gyrus.

2.9 Statistical Analyses

All data were analyzed using the statistical software program SPSS (IBM). Data for the analysis of gene expression in the brain and spleen and the protein levels of cytokines in the serum were assessed for normal distribution with the Shapiro-Wilk test and homogeneity of variance with the Levene's test followed by either a $2 \times 2 \times 2$ ANOVA, or Mann-Whitney U tests when appropriate, with Sex (male vs female), Neonatal Infection (Saline vs *E. coli*), and Time (8- vs 24-hours) as the between-subjects factors. For microglia counts, data for the number of each classification of microglia morphology and the total number of all microglia within the whole hippocampus, CA1, CA3, and the dentate gyrus were analyzed using 2×2 ANOVAs with Sex (male vs female) and Neonatal Infection (saline vs *E.coli*) as the between-subjects factors. Differences in the total number of each type of microglia morphology within the whole hippocampus were examined using a $2 \times 2 \times 4$ repeated measures ANOVA, with Sex (male vs female) and Neonatal Infection (salive vs *E.coli*) as the between-subjects factors and Microglial Morphology (round vs stout vs thick vs thin) as the within-subjects factor. All data were assessed for outliers using the interquartile range method of detecting outliers, however, no more than one statistical outlier was ever removed from one treatment group in an experiment. The accepted significance level for all analyses was $p < 0.05$. Significant interactions were followed by post hoc tests using the Bonferroni correction to examine between-group differences.

3 Results

3.1 E.coli infection increases IL-1β and IL-6 gene expression in the neonatal hippocampus of male and female rats

In the hippocampus, there was a main effect of *E.coli* infection which increased in *IL-1β* expression at 8- and 24-hours post-infection (Fig. 1A; Neonatal Infection: $F_{1,66} = 6.169$, $p = 0.016$), and a main effect of Time such that *IL-1β* expression was significantly increased at 24- hours compared to 8-hours (Fig. 1A; Time: $F_{1,66} = 21.025$, $p = 0.001$). *E.coli* infection produced a significant increase in *TNF-α* expression (interaction of Neonatal Infection x Time: $F_{1,67} = 27.738$, $p < 0.001$) and *CD11b* expression (interaction of Neonatal Infection x Time: $F_{1,68} = 5.482$, $p = 0.022$) at 8-hours post-infection relative to saline treated pups ($p < 0.001$ and $p = 0.010$, respectively; **Fig. 1C and 1D**), an effect that was not present at 24-hours post-infection. Males expressed significantly lower levels of *Iba-1* compared to females at 8-hours post-infection (interaction of Sex x Time: $F_{1,65} = 6.870$, $p = 0.011$), but not at 24-hours post-infection as indicated by post hoc tests ($p = 0.001$) and this sex difference was not affected by *E.coli* infection (Fig. 1E). No significant differences were observed for *IL-6* or *BDNF* expression between sex or following infection at either time point (**Fig. 1B and 1F**).

3.2 E.coli infection increases IL-6 expression in females and decreases BDNF expression in males in the neonatal cerebellum

In the cerebellum, *E.coli* infection produced a significant increase in *IL-6* expression at 8-hours post-infection in females only (interaction of Sex x Neonatal Infection x Time: $F_{1,66} = 4.198$, $p = 0.044$; Fig. 2B). Post hoc tests revealed that *E.coli*-treated females had significantly higher *IL-6* expression relative to control females ($p = 0.003$). *E.coli* infection

produced significant decreases in *BDNF* expression at 8-hours post-infection in males but not females (interaction of Sex x Neonatal Infection x Time: $F_{1,66} = 8.285$, $p = 0.005$; Fig. 2F), as indicated by post hoc tests ($p < 0.001$). Males expressed significantly lower levels of *Iba1* compared to females at 8-hours (interaction of Sex x Time: $F_{1,67} = 9.087$, $p = 0.004$), but not at 24-hours as indicated by post hoc tests ($p < 0.001$) and this difference was not affected by *E.coli* infection (Fig. 2E). *CD11b* expression was higher at 8-hours compared to 24-hours in males and females and was not affected by *E.coli* infection (Fig. 2D; main effect of Time: $U = 119.000$, p < 0.001). No significant differences were observed for *IL-1β* or *TNF-α* expression (**Fig. 2A and 2C**).

In the spleen, *E.coli* infection produced a significant increase in *IL-1β* and *TNF-α* expression at 8- and 24-hours post-infection (main effect of Neonatal Infection: $U = 1,083.500$, $p < 0.001$ and $U = 898.000$, $p = 0.004$, respectively), but these levels were significantly attenuated by 24-hours compared to 8-hours (main effect of Time: $U = 280.500$, $p < 0.001$ and $U = 148.000$, $p < 0.001$, respectively; **Fig. 3A and 3C**). *IL-6* expression was significantly lower at 24-hours compared to 8-hours (main effect of Time: $F_{1,65} = 6.684$, $p = 0.012$; Fig. 3B), and this difference was not affected by *E.coli* infection.

3.2 E.coli infection alters serum levels of inflammatory cytokines and chemokines in neonatal male and female rats

E.coli infection significantly increased the serum levels of the following cytokines and chemokines 8-hours post-infection: MIP-1α ($F_{1,63} = 4.496$, $p = 0.038$; Fig. 4B), MCP1 ($F_{1,61} = 12.777$, $p = 0.001$; **Fig.4C**), IP-10 ($F_{1,62} = 4.401$, $p = 0.040$; Fig. 4D), TNF-α ($F_{1,61} = 30.917$, $p < 0.001$; Fig. 4G), and IL-10 ($F_{1,62} = 33.212$, $p < 0.001$; Fig. 4H); however, the serum levels of all of these proteins returned to baseline by 24-hours post infection as indicated by post hoc tests ($p = 0.012$ and $p's < 0.001$, respectively). *E.coli* infection produced significant increases in GRO-KC at 8-hours, but levels were undetectable by 24-hours post-infection (main effect of Neonatal Infection: $U = 263.500$, $p < 0.001$; Fig. 4A). *E.coli* infection did not produce significant differences in IL-1β, but levels were significantly lower at 24-hours compared to 8-hours (main effect of Time: $F_{1,59} = 17.316$, $p < 0.001$; Fig. 4E). IL-6 was undetectable at both time points post-infection (Fig. 4F).

3.3 Microglia Counts in the Hippocampus 24-hours Post Infection

First, we examined whether the volume of each brain region (whole hippocampus, CA1, CA3, and dentate gyrus) differed between males and females or saline and *E.coli* infection. No significant differences in volume were found as a result of Sex or Infection in the whole hippocampus, CA3, or the dentate gyrus. However, we did find a main effect of Sex ($F_{1,16} = 4.644$, $p = 0.047$; male > female) and a main effect of Infection ($F_{1,16} = 6.316$, $p = 0.023$; saline > *E.coli*) on the volume of CA1. Despite this difference in volume, microglia counts in the CA1 were not significantly different when accounting for volume differences vs not accounting for volume differences; therefore, all of the data presented below represent the microglia counts that do not account for volume.

Microglia counts within each hippocampal subregion were analyzed separately for each microglial morphology classification (round, stout, thick, and thin; Fig. 5A) and for total

microglia number. On P5, we found a significant main effect of Sex on the number of thin microglia in the CA1 ($F_{1,16} = 5.603$, $p = 0.031$) such that males had significantly more thin microglia than females in the CA1, however, this sex difference was not affected by *E.coli* infection (Fig. 5B–D). No significant effects of Sex were found for any other microglial morphology or for the total number of microglia in CA3, DG, or whole hippocampus on P5. Notably, we found no main effect of Neonatal Infection on the individual microglia morphologies nor on the total number of microglia in the CA1, CA3, DG, or whole hippocampus 24 hours following infection (Fig. 5B–D).

Finally, a repeated measures ANOVA to examine differences in the number of each type of microglia morphology within the whole hippocampus revealed a significant main effect of Morphology ($F_{1,16} = 612.748$, $p < 0.001$) with stout microglia clearly being the predominant morphological classification present within the whole hippocampus in both males and females on P5 (Fig. 5E). The high proportion of stout microglia observed here concurs with the typical developmental trajectory that microglia follow within the whole rat hippocampus [2].

4   Discussion

The current experiments examined the acute neuroimmune response and microglia morphology in the brain of neonatal male and female rats following neonatal *E.coli* infection. Further, we examined changes in peripheral immune function following neonatal infection in both male and female rats. We determined that males and females have similar changes in microglia function in the hippocampus in the hours immediately following *E.coli* infection, despite previous findings that males have more microglia in the hippocampus on P4 than females. In the cerebellum, only males showed decreased *BDNF* expression and only females showed increased *IL-6* expression 8-hours post-infection. We found no significant difference in the expression of inflammatory cytokines and chemokines between males and females in the spleen and serum, which were mostly resolved on P5, 24-hours post-infection. Finally, we found no effect of *E.coli* infection on microglia cell counts on P5; however, we did find that males have more microglia with long, thin processes than females in the CA1 on P5, which was unaffected by infection on P4. This finding is consistent with previous data measured at other early postnatal ages [2,29].

In the neonatal hippocampus, we found no sex differences in the acute response to infection at either timepoint for any gene examined. *TNF-α, CD11b*, and *IL-1β* expression showed a robust increase in response to *E.coli* infection at 8-hours, which was resolved to baseline expression levels by 24-hours for *TNF-α* and *CD11b*; however, *IL-1β* expression continued to be elevated at 24-hours. While it appeared that males may be driving this IL-1β response (Fig. 1A) we were unable to find any significant interaction of Sex and Neonatal Infection, thus it may be informative to examine additional timepoints to determine whether there is a significant interaction of Sex with Neonatal Infection in the hours following *E.coli* infection that would indicate a sex difference in the response of IL-1β in the hippocampus. Given the important role that IL-1β has in learning and memory processes in the hippocampus [30], this lasting increase in *IL-1β* expression may have important consequences on downstream neuronal functioning by maintaining a heightened pro-inflammatory microenvironment in

the neonatal hippocampus that could potentiate deficits in learning and memory later in life [31–33]. Indeed, this phenomenon of early-life programming has been well-studied in many contexts and our data, in conjunction with previous data [30,34], suggest that in the context of early-life infection IL-1β may be an early catalyst for initiating increased vulnerability to learning and memory deficits later in life.

Iba-1 expression in the neonatal hippocampus was unaffected by *E.coli* infection; however, on P4 females expressed significantly more Iba-1 than males at baseline. Iba-1 is important for the production of membrane ruffling and phagocytic cups on microglia [35], which is necessary for microglial activation and for the role microglia have in supporting early brain development through processes such as promoting neurogenesis, cell survival, and synaptogenesis. Our data are consistent with previous findings that female microglia phagocytose neural progenitor cells at a higher rate than male microglia and have higher expression of several genes involved in the phagocytic pathway in the neonatal (P3) hippocampus [22]. This sex difference in *Iba-1* expression in the P4 hippocampus was unaffected by infection, was no longer apparent on P5, and there were no sex differences in inflammatory cytokine expression suggesting that this sex difference in *Iba-1* expression is reflective of sex differences in the role microglia have in early developmental processes rather than in their activational state following infection. Furthermore, we found that females have fewer microglia with long, thin processes than males in the CA1 on P5. Together, these data suggest that neonatal male and female microglia in the hippocampus have an overall different phenotype on P4 and P5 and that these characteristics could either be transient, disappearing within the first postnatal week, or highly dynamic throughout early postnatal brain development [2]. Despite the sex differences in microglia phenotype in the CA1 subregion of the hippocampus, we found that there are no sex differences in the acute inflammatory response to infection during the neonatal period at the time points we examined.

In the neonatal cerebellum, we found that *E.coli* infection produced a significant increase in *IL-6* expression in females 8 hours later, but no other cytokines were affected. Additionally, similar to the hippocampus, we found that females express significantly higher levels of *Iba-1* compared to males at baseline and this expression is unaffected by *E.coli* infection. These data support previous findings from Perez-Pouchoulen and colleagues [23] who found that females have fewer microglia with long, thin processes than males in the granule layer until P17 suggesting that female microglia have a more activated or immature phenotype than male microglia in the cerebellum at this age. Finally, *BDNF* expression was significantly decreased in males 8 hours after *E.coli* infection suggesting that males may be at a greater risk than females for decreased neuronal plasticity or deficits in neuronal differentiation, survival, or maturation in the cerebellum, acutely, in the hours following early-life infection, which could impact long-term neuronal function.

We found no effect of neonatal *E.coli* infection on the total number of microglia nor on the total number of any of the four morphological cell types examined.. Consistent with previous data, we found that the predominate microglia morphology in the neonatal hippocampus is stout. This morphology is indicative of their immature phenotype, having

recently entered the brain from the periphery as macrophage-like microglial progenitor cells during colonization [2,36–38].

In the periphery, *E.coli* infection increased *IL-1β* and *TNF-α* expression in the spleen at both time points in males and females. We are one of only a few groups to have investigated the peripheral cytokine response to infection in neonatal rats. Previous data have shown that these cytokines, particularly IL-1β, is mainly released from CD4+ T-helper cells and CD8+ cytotoxic T-cells in the spleen [39] and that the expression levels, while adequate to be considered an inflammatory response, are significantly lower compared to adult and even juvenile levels highlighting the developing state of these immune cells at this early age [40,41].

In the serum, *E.coli* infection significantly increased GRO-KC, MIP-1a, MCP1, IP-10, TNF-α, and IL-10 in males and females 8 hours post-infection. GRO-KC is most highly expressed by macrophages and neutrophils in the periphery and increased levels have been shown to inhibit oligodendrocyte migration in the developing brain [42]. As a cyclooxygenase- independent endogenous pyrogen, MIP-1α is a rapid fever inducer and activates several types of leukocytes including macrophages, monocytes, and neutrophils [43]. MCP1 and IP-10 are chemoattractants that recruit several immune cell types including monocytes and dendritic cells to the sourse of inflammation [44]. Perhaps surprisingly, IL-1β in the serum was not affected by *E.coli* infection, but was significantly decreased on P5 compared to the 8-hour time point in both males and females; however, Jessop and Hoffman [45] showed that LPS induces IL-1β release from monocytes within 3 hours, so it is possible that the 8-hour time point we examined here missed the critical window for detecting the IL-1β response from peripheral leukocytes. In this same vein, Tosato and Jones [46] found that IL-1β induces IL-6 from monocytes, but we were unable to detect any IL-6 protein at either time point again suggesting the possibility that we missed a critical window for detecting these two cytokines in the periphery of our neonatal rats. We also found that TNF-α was significantly increased in the serum 8-hours following E.coli infection. TNF-α has been shown to induce a strong sickness response in 10-week-old male mice [47] verifying that while our *E.coli* dose is not high, it is likely sufficient to produce the typical sickness response expected from this type of infection even at this early stage of development.Finally, we saw increased levels of IL-10 at the 8-hour time point. IL-10 is most highly expressed from monocytes, CD8+ and CD4+ T-cells, and increased levels of this cytokine have been shown to effectively decrease IL-1β and IL-6 faster than if IL-10 were not present [48], which may also explain the lack of changes in IL-1β and the undetectable levels of IL-6 in our data as we found an approximate 80-fold increase in IL-10 levels at the 8-hour time point.

In conclusion, we characterized the immune response in male and female rats in the time acutely following early-life infection on P4, a time when sex differences in microglia development are evident in several brain regions. We identified sex differences in the immune response to early-life infection, specifically in the cerebellum, while in the hippocampus and periphery, sex differences were either not as robust or were not evident at the time points we examined. The timepoints examined here are certainly not an exhaustive measure, therefore, in order to fully characterize the immune response to early-life infection

and determine whether sex differences are present it will be necessary to examine more ages and time courses in the hours, days, and weeks following early-life infection in both sexes. Furthermore, sex differences in the immune response following early-life infection are likely influenced by individual differences in genetics or environmental exposures which could impact how an individual responds to early-life infection and ultimately affect their risk for neurodevelopmental disorders dependent or independent of sex. Future studies should take all of these factors into consideration to develop a comprehensive understanding of the immune response to early-life infection in males and females.

Acknowledgements

Abbreviations

IL-1β	Interleukin-1β
IL-6	Interleukin-6
TNF-α	tumor necrosis factor-α
CD11b	cluster differentiation factor 11b
Iba1	ionized calcium-binding adaptor molecule 1
BDNF	brain derived neurotrophic factor
MCP-1	monocyte chemoattractant protein1
MIP-1α	monocyte inflammatory protein 1α
GRO-KC	growth-related oncogene/keratinocyte-related chemokine
IP-10	interferon-inducible protein 10
IL-10	interleukin −10
E.coli	*Escherichia* coli
CFU	colony forming units
P	postnatal day
E	embryonic day
ASD	autism spectrum disorders
RNA	ribonucleic acid

DNA	deoxynucleic acid
cDNA	complementary DNA
PCR	polymerase chain reaction
DPBS	Dulbecco's phosphate buffered saline
SPSS	Statistical Package for the Social Sciences

References

[1]. Ginhoux F, Prinz M, Origin of Microglia: Current Concepts and Past Controversies, Cold Spring Harb. Perspect. Biol 15 (2015). doi:10.1101/cshperspect.a020537.

[2]. Schwarz JM, Sholar PW, Bilbo SD, Sex differences in microglial colonization of the developing rat brain, J. Neurochem 193 (2012) 118–125. doi:10.1016/j.jneumeth.2010.08.011.Autogenic.

[3]. Lenz KM, Nugent BM, Haliyur R, McCarthy MM, Microglia Are Essential to Masculinization of Brain and Behavior, J. Neurosci 33 (2013) 2761–2772. doi:10.1523/JNEUROSCI.1268-12.2013. [PubMed: 23407936]

[4]. Schafer DP, Stevens B, Phagocytic Glial Cells: Sculpting Synaptic Circuits in the Developing Nervous System, Curr. Opin. Neurobiol 23 (2013) 1034–1040. doi:10.1016/j.conb.2013.09.012. [PubMed: 24157239]

[5]. Nikodemova M, Kimyon RS, De I, Small AL, Collier LS, Watters JJ, Microglial numbers attain adult levels after undergoing a rapid decrease in cell number in the third postnatal week., J. Neuroimmunol 278 (2015) 280–8. doi:10.1016/j.jneuroim.2014.11.018. [PubMed: 25468773]

[6]. Kingham PJ, Cuzner ML, Pocock JM, Apoptotic Pathways Mobilized in Microglia and Neurones as a Consequence of Chromogranin A-Induced Microglial Activation, J. Neurochem 73 (2002) 538–547. doi:10.1046/j.1471-4159.1999.0730538.x.

[7]. Polazzi E, Contestabile A, Reciprocal interactions between microglia and neurons: from survival to neuropathology., Rev. Neurosci 13 (2002) 221–42. http://www.ncbi.nlm.nih.gov/pubmed/12405226 (accessed September 18, 2018). [PubMed: 12405226]

[8]. Marín-Teva JL, Dusart I, Colin C, Gervais A, van Rooijen N, Mallat M, Microglia promote the death of developing Purkinje cells., Neuron 41 (2004) 535–47. doi:10.1016/S0896-6273(04)00069-8. [PubMed: 14980203]

[9]. Mallat M, Luis Marín-Teva J, Ché Ret C, Phagocytosis in the developing CNS: more than clearing the corpses, Curr. Opin. Neurobiol 15 (2005) 101–107. doi:10.1016/j.conb.2005.01.006. [PubMed: 15721751]

[10]. Tremblay M-È, Stevens B, Sierra A, Wake H, Bessis A, Nimmerjahn A, The role of microglia in the healthy brain., J. Neurosci 31 (2011) 16064–9. doi:10.1523/JNEUROSCI.4158-11.2011. [PubMed: 22072657]

[11]. Hong S, Dissing-Olesen L, Stevens B, New insights on the role of microglia in synaptic pruning in health and disease This review comes from a themed issue on Neurobiology of disease, Curr. Opin. Neurobiol 36 (2016) 128–134. doi:10.1016/j.conb.2015.12.004. [PubMed: 26745839]

[12]. Salter MW, Beggs S, Sublime Microglia: Expanding Roles for the Guardians of the CNS, Cell 158 (2014) 15–24. doi:10.1016/j.cell.2014.06.008. [PubMed: 24995975]

[13]. Tay TL, Savage JC, Hui CW, Bisht K, Tremblay M-È, Microglia across the lifespan: from origin to function in brain development, plasticity and cognition, J. Physiol 595 (2017) 1929–1945. doi:10.1113/JP272134. [PubMed: 27104646]

[14]. Paolicelli RC, Bolasco G, Pagani F, Maggi L, Scianni M, Panzanelli P, Giustetto M, Ferreira TA, Guiducci E, Dumas L, Ragozzino D, Gross CT, Synaptic Pruning by Microglia Is Necessary for Normal Brain Development, Science (80-.) 333 (2011). http://science.sciencemag.org/content/sci/333/6048/1456.full.pdf (accessed May 5, 2017).

[15]. Laskaris LE, Di Biase MA, Everall I, Chana G, Christopoulos A, Skafidas E, Cropley VL, Pantelis C, Microglial activation and progressive brain changes in schizophrenia, Br. J. Pharmacol 173 (2016) 666–680. doi:10.1111/bph.13364. [PubMed: 26455353]

[16]. Yirmiya R, Rimmerman N, Reshef R, Depression as a Microglial Disease, Trends Neurosci 38 (2015) 637–658. doi:10.1016/j.tins.2015.08.001. [PubMed: 26442697]

[17]. Insel TR, Landis SC, Twenty-five years of progress: The view from NIMH and NINDS, Neuron 80 (2013) 561–567. doi:10.1016/j.neuron.2013.09.041. [PubMed: 24183009]

[18]. MacLusky N, Naftolin F, The hormonal control of sexual development., Science (80-.) 211 (1981) 1278–84. doi:10.1126/science.7010602.

[19]. Arnold AP, Gorski RA, Gonadal Steroid Induction of Structural Sex Differences in the Central Nervous System, Annu. Rev. Neurosci 7 (1984) 413–442. doi:10.1146/annurev.ne. 07.030184.002213. [PubMed: 6370082]

[20]. Arnold AP, Breedlove M, Organizational and Activational Effects of Sex Steroids on Brain and Behavior: A Reanalysis, 1985 https://ac-els-cdn- com.udel.idm.oclc.org/0018506X8590042X/1- s2.0-0018506X8590042X- main.pdf?_tid=ea7eb531-5bbf-4f21-8a15- feabb602c756&acdnat=1537313995_f8500eb7fc24bdc1addb7a16bda02f0f (accessed September 18, 2018).

[21]. Mccarthy MM, Wright CL, Schwarz JM, New tricks by an old dogma: Mechanisms of the Organizational / Activational Hypothesis of steroid-mediated sexual differentiation of brain and behavior, Horm. Behav 55 (2009) 655–665. doi:10.1016/j.yhbeh.2009.02.012. [PubMed: 19682425]

[22]. Nelson LH, Warden S, Lenz KM, Sex differences in microglial phagocytosis in the neonatal hippocampus, Brain. Behav. Immun 64 (2017) 11–22. doi:10.1016/j.bbi.2017.03.010. [PubMed: 28341582]

[23]. Perez-pouchoulen M, Vanryzin JW, Mccarthy MM, Morphological and Phagocytic Profile of Microglia in the Developing Rat Cerebellum 1 , 2 , 3, ENeuro 2 (2015) 1–15. doi:10.1523/ ENEURO.0036-15.2015.

[24]. Frick LR, Williams K, Pittenger C, Microglial dysregulation in psychiatric disease, Clin. Dev. Immunol 2013 (2013). doi:10.1155/2013/608654.

[25]. O'connor TG, Moynihan JA, Caserta MT, Annual Research Review: The neuroinflammation hypothesis for stress and psychopathology in children: developmental psychoneuroimmunology, J Child Psychol Psychiatry 55 (2014) 615–631. doi:10.1111/jcpp.12187. [PubMed: 24372371]

[26]. Maezawa I, Calafiore M, Wulff H, Jin L-W, Glia N, Author B, Does microglial dysfunction play a role in autism and Rett syndrome? HHS Public Access Author manuscript, Neuron Glia Biol 7 (2011) 85–97. doi:10.1017/S1740925X1200004X. [PubMed: 22717189]

[27]. Schwarz JM, Bilbo SD, Sex, glia, and development: Interactions in health and disease, Horm. Behav 62 (2012) 243–253. doi:10.1016/j.yhbeh.2012.02.018. [PubMed: 22387107]

[28]. McCarthy MM, Wright CL, Convergence of Sex Differences and the Neuroimmune System in Autism Spectrum Disorder., Biol. Psychiatry 81 (2017) 402–410. doi:10.1016/j.biopsych. 2016.10.004. [PubMed: 27871670]

[29]. Nelson LH, Lenz KM, The immune system as a novel regulator of sex differences in brain and behavioral development, J. Neurosci. Res 95 (2017) 447–461. doi:10.1002/jnr.23821. [PubMed: 27870450]

[30]. Williamson LL, Sholar PW, Mistry RS, Smith SH, Bilbo SD, Microglia and Memory: Modulation by Early-Life Infection, J. Neurosci 31 (2011) 15511–15521. doi:10.1523/ JNEUROSCI.3688-11.2011. [PubMed: 22031897]

[31]. Bilbo SD, Early-life programming of later-life brain and behavior: a critical role for the immune system, Front. Behav. Neurosci 3 (2009) 1–14. doi:10.3389/neuro.08.014.2009. [PubMed: 19194528]

[32]. Bilbo SD, Schwarz JM, The immune system and developmental programming of brain and behavior, Front. Neuroendocrinol 33 (2012) 267–286. doi:10.1016/j.yfrne.2012.08.006. [PubMed: 22982535]

[33]. Barker DJ, Gluckman PD, Robinson JS, Conference report: fetal origins of adult disease--report of the First International Study Group, Sydney, 29–30 October 1994., Placenta 16 (1995) 317–20. doi:10.1016/0143-4004(95)90118-3. [PubMed: 7638112]

[34]. Bilbo SD, Biedenkapp JC, Der-Avakian A, Watkins LR, Rudy JW, Maier SF, Neonatal Infection-Induced Memory Impairment after Lipopolysaccharide in Adulthood Is Prevented via Caspase-1 Inhibition, J. Neurosci 25 (2005) 8000–8009. doi:10.1523/JNEUROSCI.1748-05.2005. [PubMed: 16135757]

[35]. Ohsawa K, Yoshinori I, Kanazawa H, Sasaki Y, Kohsaka S, Involvement of Iba1 in membrane ruffling and phagocytosis of macrophages/microglia, J. Cell Sci 113 (2000) 3073–3084. http://jcs.biologists.org.udel.idm.oclc.org/content/joces/113/17/3073.full.pdf (accessed September 18, 2018). [PubMed: 10934045]

[36]. Male D, Rezaie P, Colonisation of the human central nervous system by microglia: the roles of chemokines and vascular adhesion molecules Colonisation of the central nervous system (CNS) by microglia, in: Prog. Bruin Res, 2001: pp. 81–93. https://ac-els-cdn- com.udel.idm.oclc.org/S0079612301320678/1-s2.0-S0079612301320678- main.pdf?_tid=f9a3f57c-d139-4b72-8821-1f7262fefa30&acdnat=1537315037_e3f0a2951263f8e299791e0bf5d430ae (accessed September 18, 2018).

[37]. Rezaie P, Patel K, Male DK, Microglia in the human fetal spinal cord-patterns of distribution, morphology and phenotype, 1999 https://ac-els-cdn- com.udel.idm.oclc.org/S0165380699000437/1-s2.0-S0165380699000437- main.pdf?_tid=66bb6d01-63eb-4f7d-8750-5bd7400fcea8&acdnat=1537315108_cb92c65565b85332b30e3daef903793b (accessed September 18, 2018).

[38]. Cuadros M. a., Navascues J, The Origin and Differentiation of Microglial Cells During Development, Prog. Neurobiol 56 (1998) 173–189. [PubMed: 9760700]

[39]. Sewald K, Mueller M, Buschmann J, Hansen T, Lewin G, Development of hematological and immunological characteristics in neonatal rats, Reprod. Toxicol 56 (2015) 109–117. doi:10.1016/j.reprotox.2015.05.019. [PubMed: 26055945]

[40]. Levin D, Gershon H, IL-I Secretion and Membrane IL-l Expression by Neonatal Spleen Cells during Soluble Antigen Presentation, 1988 https://ac-els-cdn- com.udel.idm.oclc.org/0008874988902390/1-s2.0-0008874988902390- main.pdf?_tid=91db1f41-eff9-4f85-aad2-8d7f71ba906a&acdnat=1537320374_904e9c81e858365cadead33143616eb8 (accessed September 18, 2018).

[41]. Osborne BF, Caulfield JI, Solomotis SA, Schwarz JM, Neonatal infection produces significant changes in immune function with no associated learning deficits in juvenile rats, Dev. Neurobiol 77 (2017) 1221–1236. doi:10.1002/dneu.22512. [PubMed: 28719141]

[42]. Vries MHM, Allard W Verbruggen Sanne, E.L., Molin DGM, Post MJ, CXCL1 promotes arteriogenesis through enhanced monocyte recruitment into the peri-collateral space, Angiogenesis 18 (2015) 163–171. doi:10.1007/s10456-014-9454-1. [PubMed: 25490937]

[43]. Davatelis G, Wolpe SD, Sherry B, Dayer JM, Chicheportiche R, Cerami A, Macrophage inflammatory protein-1: a prostaglandin-independent endogenous pyrogen., Science 243 (1989) 1066–8. doi:10.1126/SCIENCE.2646711. [PubMed: 2646711]

[44]. Carr MW, Rothtt SJ, Luthert# ED, Roseti SS, Springer TA, T-lymphocyte chemoattractant, 1994 http://www.pnas.org.udel.idm.oclc.org/content/pnas/91/9/3652.full.pdf (accessed September 18, 2018).

[45]. Jessop JJ, Hoffman T, Production and release of IL-1 beta by human peripheral blood monocytes in response to diverse stimuli: possible role of "microdamage" to account for unregulated release., Lymphokine Cytokine Res 12 (1993) 51–8. http://www.ncbi.nlm.nih.gov/pubmed/8457632 (accessed September 18, 2018). [PubMed: 8457632]

[46]. Giovanna Tosato B, Jones KD, Interleukin-1 Induces Interleukin-6 Production in Peripheral Blood Monocytes, 1990 www.bloodjournal.org (accessed September 18, 2018).

[47]. Biesmans S, Bouwknecht J, Ver Donck L, Langlois X, Acton P, et al P. De Haes, Peripheral Administration of Tumour Necrosis Factor-Alpha Induces Neuroinflammation and Sickness but Not Depressive-Like Behavior in Mice, Biomed Res. Int 2015 (2015) 716920. [PubMed: 26290874]

[48]. Krzyszton CP, Sparkman NL, Grant RW, Buchanan JB, Broussard SR, Woods J, Johnson RW, Exacerbated fatigue and motor deficits in interleukin-10-deficient mice after peripheral immune stimulation, Am J Physiol Regul Integr Comp Physiol 295 (2008) 1109–1114. doi:10.1152/ajpregu.90302.2008.

Highlights

- Females have higher Iba-1 expression than males in the hippocampus and cerebellum

- Neonatal infection increases IL-6 expression in the neonatal female cerebellum

- Neonatal infection decreases BDNF expression in the neonatal male cerebellum

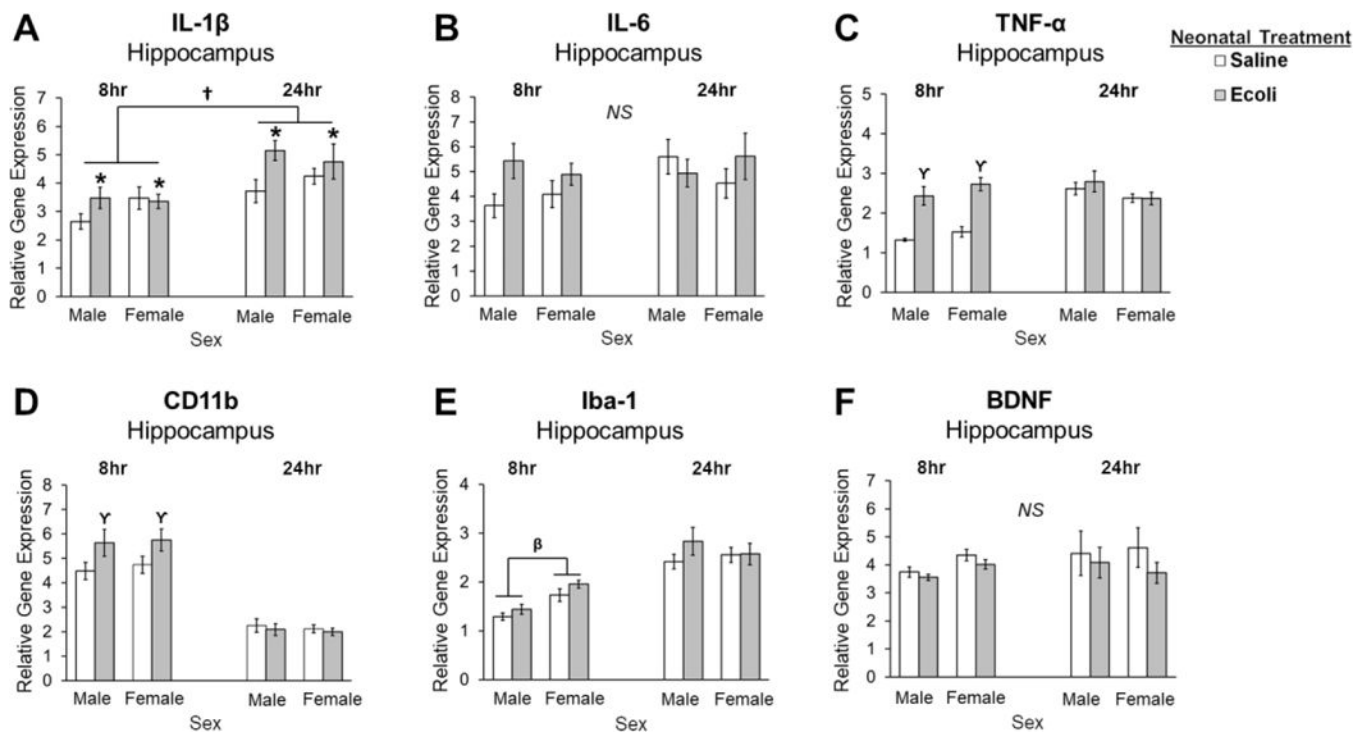- Neonatal infection increases peripheral cytokines and chemokines in both sexes

Figure 1. Impact of E.coli (1×10^6 CFU/0.1mL/kg) in the hippocampus of male and female neonates 8- and 24-hours following infection.

(A) Relative gene expression of the proinflammatory cytokine IL-1β is significantly increased in males and females following neonatal infection at both time points, and is significantly increased at 24 hours post-infection compared to 8 hours. **(B)** Relative gene expression of the proinflammatory cytokine IL-6 is not significantly different following neonatal infection at either time point in males or females. **(C)** Relative gene expression of the proinflammatory cytokine TNF-α is increased in males and females following neonatal infection at 8 hours, but not 24 hours post-infection. **(D)** Relative gene expression of a marker of microglial activation, CD11b, is significantly increased in males and females 8 hours post-infection but not at 24 hours. **(E)** Relative gene expression of Iba-1 is lower in males compared to females at 8 hours, but not at 24 hours post-infection. **(F)** Relative gene expression of the trophic factor, BDNF, is not significantly different following neonatal infection at either time point in males or females. Error bars represent ±SEM. $^{*}p < 0.05$ represents the main effect of Neonatal Treatment. $^{\dagger}p < 0.05$ represents the main effect of Time. $^{\Upsilon}p < 0.05$ represents a significant interaction of Neonatal Treatment and Time. $^{\beta}p < 0.05$ represents a significant interaction of Sex and Time.
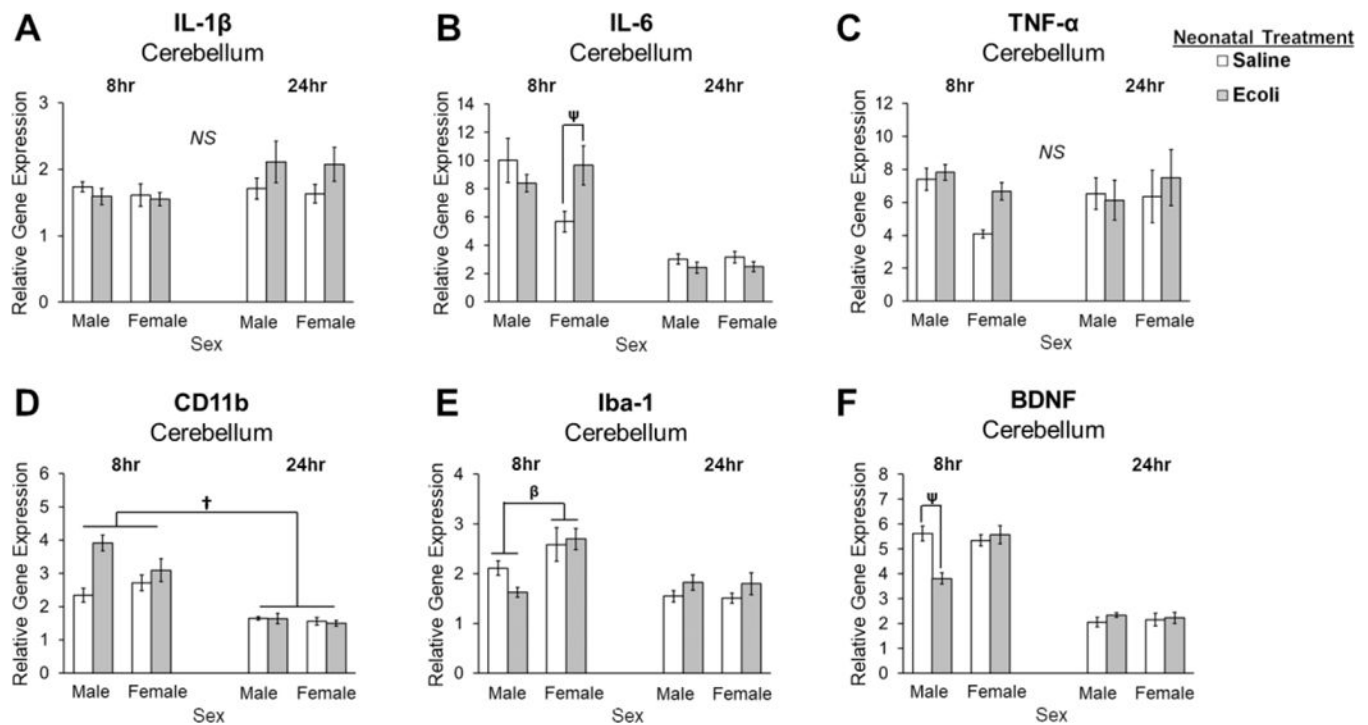
Figure 2. Impact of *E.coli* (1×10^6 CFU/0.1mL/kg) in the cerebellum of male and female neonates 8- and 24-hours following infection.
(A) Relative gene expression of the proinflammatory cytokine IL-1β is not significantly different in males or females following neonatal infection at either time point. **(B)** Relative gene expression of the proinflammatory cytokine IL-6 is significantly increased in females 8 hours post-infection. **(C)** Relative gene expression of the proinflammatory cytokine TNF-α is not significantly different in males or females following neonatal infection at either time point. **(D)** Relative gene expression of a marker of microglial activation, CD11b, is significantly greater at 8 hours compared to 24 hours. **(E)** Relative gene expression of Iba-1 is lower in males compared to females at 8 hours, but not at 24 hours post-infection. **(F)** Relative gene expression of the trophic factor, BDNF, is significantly decreased in males following neonatal infection at 8 hours. Error bars represent ±SEM. †$p < 0.05$ represents the main effect of Time. β$p < 0.05$ represents a significant interaction of Sex and Time. Ψ$p < 0.05$ represents a significant interaction of Sex, Neonatal Treatment, and Time.
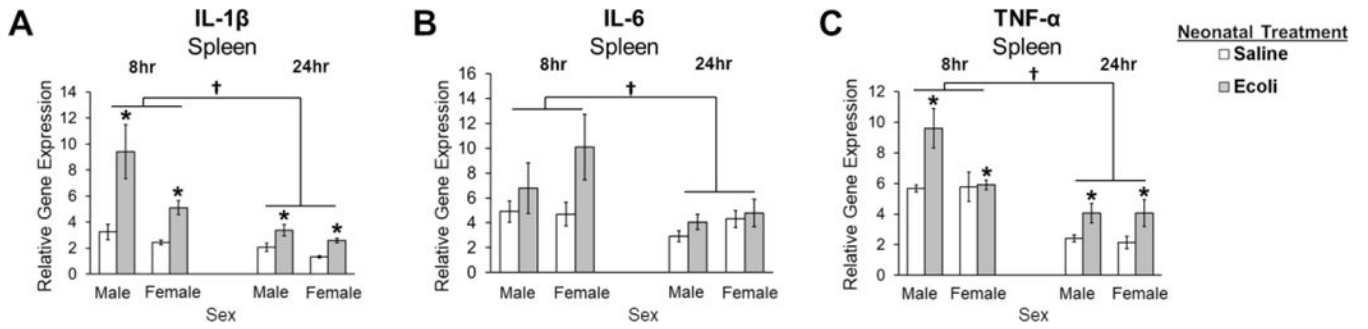
Figure 3. Impact of *E.coli* (1×10^6 CFU/0.1mL/kg) in the spleen of male and female neonates 8- and 24-hours following infection.

(A) Relative gene expression of the proinflammatory cytokine IL-1β is significantly increased in males and females following neonatal infection at both time points, but is significantly decreased at 24 hours post-infection compared to 8 hours. **(B)** Relative gene expression of the proinflammatory cytokine IL-6 is not significantly affected by neonatal infection and is significantly lower at 24 hours post-infection compared to 8 hours in males and females. **(C)** Relative gene expression of the proinflammatory cytokine TNF-α is increased in males and females following neonatal infection at both time points, but is significantly decreased at 24 hours post-infection compared to 8 hours. Error bars represent ±SEM. $^*p < .05$ represents the main effect of Neonatal Treatment. $^{†}p < 0.05$ represents the main effect of Time.
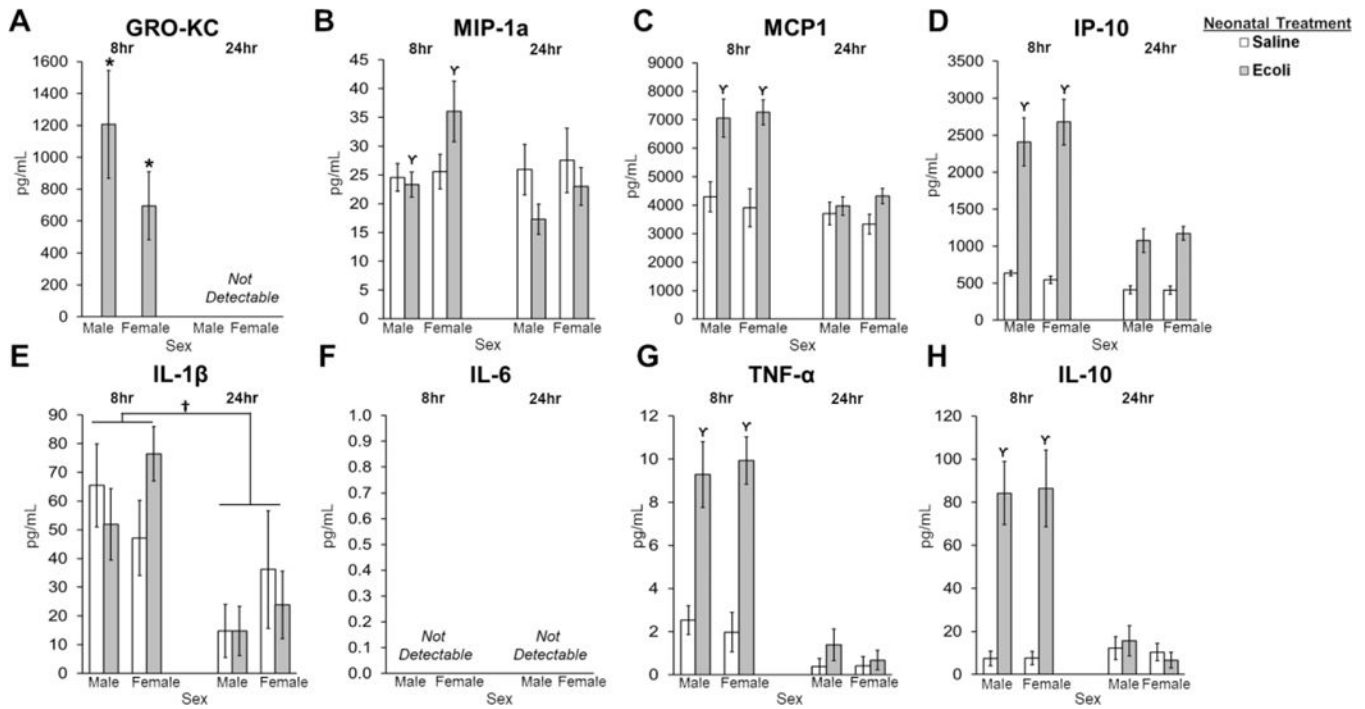
Figure 4. Impact of *E.coli* (1×10^6 CFU/0.1mL/kg) on peripheral immune response in the serum of male and female neonates 8- and 24-hours following infection.

(**A**) GRO-KC levels are significantly increased in males and females following neonatal infection at 8 hours post-infection, but levels are not detectable by 24 hours. (**B**) MIP-1a levels are significantly increased in males and females infected with *E.coli* 8 hours post-infection compared to 24 hours. (**C**) MCP1 levels are significantly increased in males and females infected with *E.coli* 8 hours post-infection compared to 24 hours. (**D**) IP-10 levels are significantly increased in males and females infected with *E.coli* 8 hours post-infection compared to 24 hours. (**E**) IL-1β levels are significantly higher 8 hours post-infection compared to 24 hours. (**F**) IL-6 levels were not detectable at 8 or 24 hours post-infection. (**G**) TNF-α levels are significantly increased in males and females infected with *E.coli* 8 hours post-infection compared to 24 hours. (**H**) IL-10 levels are significantly increased in males and females infected with *E.coli* 8 hours post-infection compared to 24 hours. Error bars represent ±SEM. $^*p < 0.05$ represents the main effect of Neonatal Treatment. $^\dagger p < 0.05$ represents the main effect of Time. $^\Upsilon p < 0.05$ represents a significant interaction of Neonatal Treatment and Time.
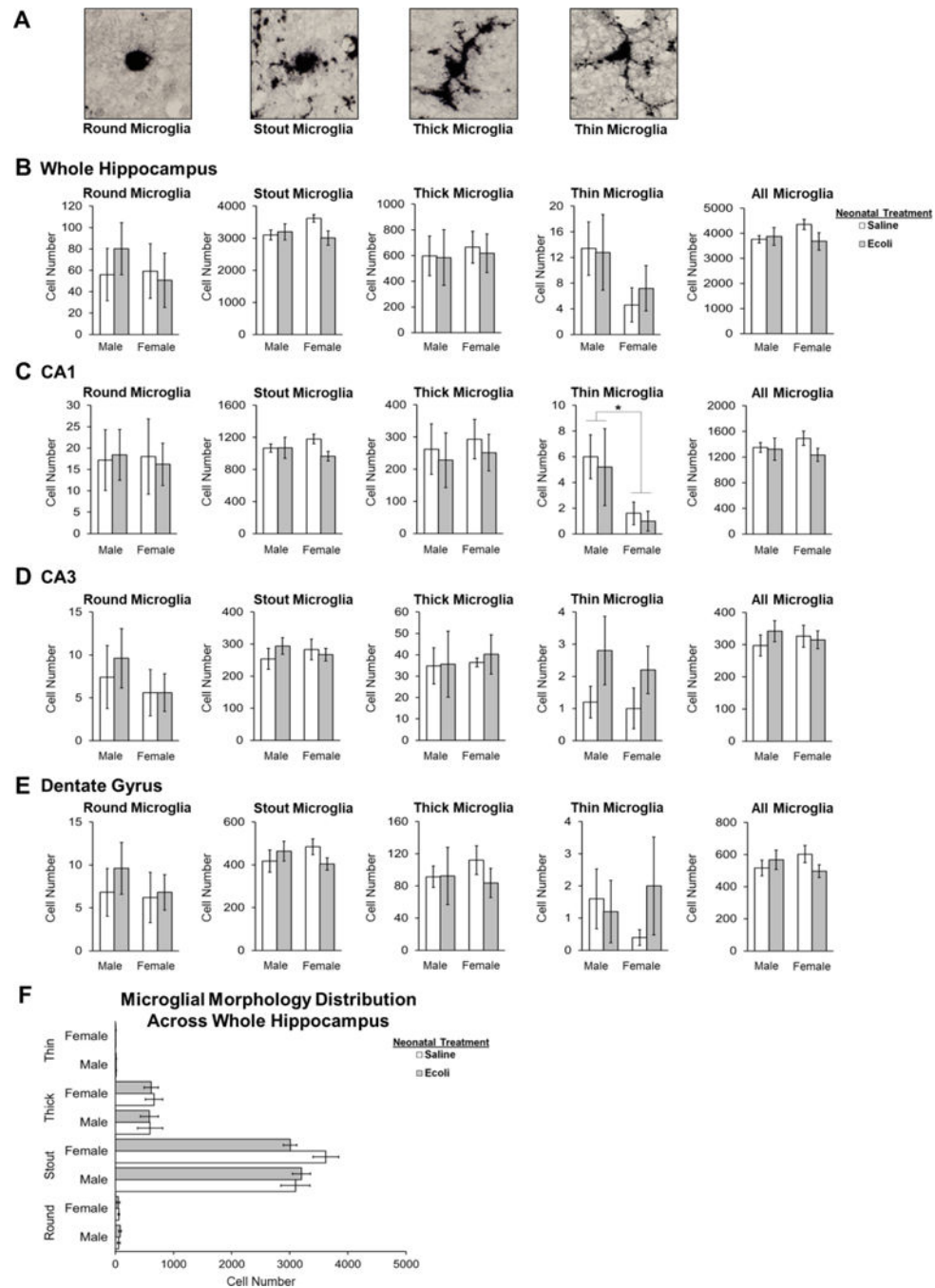
Figure 5. Microglia Counts in the hippocampus 24-hours Post Infection.
(**A**) Representative images of the four microglial phenotypes (round, stout, thick, thin) found in the hippocampus on P5 (**B**) There are no significant differences in microglia number in the whole hippocampus 24-hours post infection. (**C**) Males have significantly more thin microglia than females in the CA1 region on P5. (**D**) There are no significant differences in microglia number in the CA3 region 24-hours post infection. (**E**) There are no significant differences in microglia number in the dentate gyrus 24-hours post infection. (**F**) There are

significantly more stout microglia in the hippocampus on P5 relative to all other microglial morphologies. Error bars represent ±SEM. *$p < 0.05$.

Table 1.

Rat primers used in the current experiments for quantitative real-time PCR.

Gene	NCBI Sequence	Primers
GAPDH	NM_017008	F: GTTTGTGATGGGTGTGAACC R: TCTTCTGAGTGGCAGTGATG
CD11b	NM_012711.1	F: CTGGGAGATGTGAATGGAG R:ACTGATGCTGGCTACTGATG
IL-1β	NM_031512.2	F: GAAGTCAAGACCAAAGTGG R: TGAAGTCAACTATGTCCCG
TNF-α	NM_012675.3	F: CTTCAAGGGACAAGGCTG R: GAGGCTGACTTTCTCCTG
Iba-1	NM_017196.3	F: GAATGATGCTGGGCAAGAGA R: CAGTTGGCTTCTGGTGTTC
BDNF	NM_001270638.1	F: ATCCCATGGGTTACACGAAGGAAG R: AGTAAGGGCCCGAACATACGATTG